IVYSPRING INTERNATIONAL PUBLISHER

Theranostics

2017; 7(15): 3690-3699. doi: 10.7150/thno.18345

Research Paper

Preclinical activity of DCZ3301, a novel aryl-guanidino compound in the therapy of multiple myeloma

Minjie Gao[1*], Bo Li[2*], Xi Sun[1*], Yunfei Zhou[2], Yingcong Wang[1],Van S. Tompkins[3], Zhijian Xu[2], Nekitsing Indima[4], Houcai Wang[1], Wenqin Xiao[1], Lu Gao[1], Gege Chen[1], Huiqun Wu[1], Xiaosong Wu[1], Yuanyuan Kong[1], Bingqian Xie[1], Yiwen Zhang [1], Gaomei Chang[1], Liangning Hu[1], Guang Yang[1], Bojie Dai[5], Yi Tao[1]✉, Weiliang Zhu[2]✉ and Jumei Shi[1]✉

1. Department of Hematology, Shanghai Tenth People's Hospital, Tongji University Cancer Center, Tongji University School of Medicine, Shanghai 200072, China;
2. CAS Key Laboratory of Receptor Research, Drug Discovery and Design Center, Shanghai Institute of Materia Medica, Chinese Academy of Sciences, Shanghai 201203, China;
3. Biochemistry, Biophysics, and Molecular Biology Department, Iowa State University, Ames, IA, USA;
4. Department of Radiology, Shanghai Tenth People's Hospital, Tongji University School of Medicine, Shanghai 200072, China;
5. College of life science and technology, Tongji University, Shanghai 200092, China.

* These authors contributed equally to this work.

✉ Corresponding authors: Jumei Shi, Department of Hematology, Shanghai Tenth People's Hospital, Tongji University School of Medicine, 301 Yanchang Road, Shanghai 200072, China; Phone: +86-021-66306764; E-mail: shijumei@tongji.edu.cn and Weiliang Zhu, CAS Key Laboratory of Receptor Research, Drug Discovery and Design Center, Shanghai Institute of Materia Medica, Chinese Academy of Sciences, 555 Zuchongzhi Road, Shanghai 201203, China; Phone: +86-021-50805020; E-mail: wlzhu@simm.ac.cn and Yi Tao, Department of Hematology, Shanghai Tenth People's Hospital, Tongji University School of Medicine, 301 Yanchang Road, Shanghai 200072, China; Phone: +86-021-66306765; E-mail: taoyi018@139.com

Received: 2016.11.14; Accepted: 2017.07.17; Published: 2017.08.23

Abstract

We synthesized a novel aryl-guanidino compound, DCZ3301, and found that it has potent cytotoxicity against multiple human cancer cell lines. The anticancer activity was most potent against multiple myeloma (MM). DCZ3301 induced cytotoxicity in MM cell lines, as well as patient myeloma cells, in part by decreasing mitochondrial membrane potential to induce apoptosis. In contrast, DCZ3301 had no cytotoxic effect on normal cells. DCZ3301 also inhibited cell cycling and caused a G2/M accumulation that corresponded with downregulation of Cdc25C, CDK1, and Cyclin B1. DCZ3301 retained its activity against MM cells in the presence of exogenous cytokines (IL-6 or VEGF) or bone marrow stromal cells (BMSCs) and reduced activity of multiple signaling pathways (STAT3, NFκB, AKT, ERK1/2) in MM but not normal cells. The STAT3 pathway played an important role in modulating DCZ3301-mediated cytotoxicity. Knockdown of STAT3 using siRNA in MM cells enhanced DCZ3301-induced cytotoxicity, whereas overexpression of STAT3 in MM cells partially protected them from apoptosis. In addition, DCZ3301 inhibited VEGF and IL-6 secretion in a dose-dependent fashion in a co-culture of MM cells and BMSCs. Combining DCZ3301 with bortezomib induced synergistic cytotoxicity in MM cell lines and primary MM cells. Finally, *in vivo* efficacy of DCZ3301 was confirmed in an MM xenograft mouse model. Together, these results provide a rationale for translation of this small-molecule inhibitor, either alone or in combination, to the clinic against MM.

Key words: Multiple Myeloma; DCZ3301; antitumor activities; synergistic cytotoxicity

Introduction

Multiple myeloma (MM) is a B-lineage cancer characterized by the accumulation of clonal plasma cells predominantly in bone marrow (BM)[1, 2]. MM accounts for 1% of all cancers and approximately 10% of all hematologic cancers[3]. Despite current available treatments, including immunomodulatory drugs[4], proteasome inhibitors[5], and autologous transplantation[6, 7] that result in increased overall

survival of patients, MM remains incurable in many cases underscoring the need for novel therapeutics.

It is well known that MM is a bone marrow microenvironment-dependent tumor and that MM cell growth is regulated by bone marrow stromal cells (BMSCs)[8]. These cells secrete numerous cytokines, such as vascular endothelial growth factor (VEGF), insulin-like growth factor (IGF)-1, and interleukin (IL)-6, which are associated with MM proliferation and survival[2]. These cytokines bind with receptor tyrosine kinases to initiate tyrosine kinase signaling and trigger activation of downstream signaling pathways. Indeed, deregulation of the Raf/MEK/ERK1/2[9], the phosphoinositide 3-kinase (PI3K)/AKT[10], and the JAK2/STAT3 signaling[11] pathways frequently occurs in MM and contributes to uncontrolled proliferation and resistance to apoptosis in MM cells. These signaling pathways have been shown to be regulated by tyrosine kinases[12].

Making use of a compound library in our lab, we searched for novel molecules to treat cancer cell lines through cell-based *in vitro* screening. We discovered a novel aryl-guanidino compound, DCZ3301, and found that it has potent anti-tumor activity against MM cells. We further examined the anti-MM activities of DCZ3301 *in vitro* and using a MM xenograft model. DCZ3301 induced cytotoxicity in MM cell lines and patient MM cells, at concentrations that are not cytotoxic to normal cells. Importantly, DCZ3301 overcame the protective effect of the BM microenvironment on MM cells, and demonstrated anti-tumor activity in an MM xenograft model. DCZ3301 also synergized with bortezomib in MM cell lines and primary MM cells. Aryl-guanidino compounds are known to inhibit tyrosine kinases, so we also explored the activity of DCZ3301 on multiple signaling pathways relevant to MM (JAK2/STAT3, NFκB, AKT, ERK1/2) and revealed a multi-modal mechanism for DCZ3301.

Materials and Methods

Reagents

DCZ3301 (purity > 98%) was synthesized by Shanghai Institute of Materia Medica, Chinese Academy of Sciences, Shanghai, China. This compound has been patented and the relevant patent number is 2016102204055 recorded by State Intellectual Property Office Of The P.R.C. DCZ3301 was dissolved in dimethyl sulfoxide (DMSO; Sigma, St. Louis, MO, USA) at a concentration of 16 mmol/L (16 mM) and stored at -20°C until use. IL-6 and VEGF were purchased from R&D Systems (Minneapolis, MN, USA). Human CD138 MicroBead was obtained from Miltenyi (Miltenyi Biotec GmbH, Germany). Antibodies for caspase 3, 8, and 9, PARP, ERK1/2, AKT, STAT3, phospho(p)-ERK1/2, p-AKT, p-STAT3, β-actin were purchased from Cell Signaling Technology; Cdc25C, CDK1, Cyclin B1, IKBα, p-IKBα(Ser32), p-p65(S536) were from Abcam. Z-VAD-FMK was provided by Selleck Chemicals (Houston, TX, USA). Cell Counting Kit-8 (CCK-8) was obtained from Dojindo. Annexin V-FITC and PI detection kit was purchased from BD Pharmingen (San Diego, CA). Mitochondrial membrane potential assay kit with JC-1 was obtained from Beyotime Institute of Biotechnology.

Cell culture

Human MM cell lines MM.1S, NCI-H929 and RPMI-8226 were purchased from the American Type Culture Collection (ATCC; Manassas, VA, USA) and genotyped by the company. Human MM cell lines (U266, OCI-My5, OPM2, ARP1 and 8226-R5), human hepatocellular carcinoma cell lines (LM3 and BEL7402), thyroid carcinoma cell lines (SW1736 and K1), renal clear cell carcinoma cell line 786-0, T-cell leukemia cell line MOLT-4 and lymphoma cell NUDUL-1 were purchased from cell resource center of Shanghai institute of biological sciences (Shanghai, China). MM, T-cell leukemia and lymphoma cell lines were cultured in RPMI-1640 medium. Human hepatocellular carcinoma, thyroid carcinoma and renal clear cell carcinoma cell lines were cultured in DMEM medium. These medium contained 10% fetal bovine serum (FBS, Sigma Chemical Co., St. Louis, MO, USA), 100 IU/mL penicillin and 100 μg/mL streptomycin (GIBCO, Grand Island, NY, USA).

Primary cells

Bone marrow samples were obtained from MM patients after informed consent was obtained in accordance with the Declaration of Helsinki protocol and approval by the Institutional Review Board of Shanghai Tenth People's Hospital, Tongji University. Bone marrow mononuclear cells (BMMCs) were separated by Ficoll-Hypaque density gradient centrifugation, and plasma cells were purified (>95% $CD138^+$) using Human CD138 MicroBeads (Miltenyi Biotech, Auburn, CA). BMSCs were generated by culturing BMMCs in DMEM medium containing 15% FBS, 100 IU/mL penicillin and 100 μg/mL streptomycin for 4 to 6 weeks. Blood samples were collected from healthy volunteers and processed by Ficoll-Hypaque density gradient centrifugation to obtain peripheral blood mononuclear cells (PBMCs).

BCR stimulation

Freshly isolated PBMCs were enriched in CD19+ B cells using Human CD19 MicroBeads (Miltenyi

Biotech, Auburn, CA). B lymphocytes were cultured in 96-well plates at 5 × 10^5 cells/well in RPMI 1640 medium supplemented with 10% heat-inactivated FBS, 0.3 mg/mL l-glutamine, 100 IU/mL penicillin and 100 μg/mL streptomycin. BCR stimulation was performed by adding a $F(ab')_2$ goat anti–human IgM (Sigma-Aldrich) at a final concentration of 10 μg/mL for 24 h. After that, cells were treated with DCZ3301 (0-32_μM) for 48 h, then cell proliferation rate was assessed by CCK-8.

Growth Inhibition assay

The growth inhibitory effect of DCZ3301 on MM cell lines, patient MM cells, normal BMMCs, and PBMCs was assessed by using CCK-8 kit, as previously described[13]. To evaluate the effect of DCZ3301 on MM cell growth in the presence of BMSC or cytokine (IL-6 or VEGF), MM.1S cells (2×10^4 cells/well) were cultured with or without BMSCs or cytokine (IL-6 and VEGF) for 48 h, in the presence or absence of DCZ3301. The rate of DNA synthesis was measured by [^{3}H]-thymidine uptake.

Cell cycling

DCZ3301-treated and –untreated MM cells were harvested, washed with PBS, and fixed with cold 70% ethanol overnight at -20°C. After that, cells were washed with PBS and then stained with 500 μl of PI/RNase staining buffer (BD) for 15 min at room temperature in the dark before flow cytometric analysis.

Apoptosis assay

Apoptosis was measured using annexin V-FITC and PI detection kit, as previously described[14]. In our studies, apoptotic cells included early (annexin V positive and PI negative) and late (both annexin V and PI positive) apoptosis.

Analysis of mitochondrial membrane potential

Mitochondrial membrane potentials (ΔΨm) were measured using JC-1 dye (Beyotime Institute of Biotechnology), as previously described[13]. Briefly, MM cells were incubated with JC-1 working solution at 37°C for 20 min, washed with JC-1 staining buffer and analyzed by flow cytometry.

Western Blot Analysis

After treatment with DCZ3301, MM cells were harvested and lysed using lysis buffer (100 mM Tris-HCl, pH 6.8, 4% SDS, 20% glycerol) at 4°C for 30 min. Total cell lysates (30 μg per lane) were subjected to SDS-PAGE separation and transferred to nitrocellulose membranes. The membranes were blocked with 5% skim milk at room temperature for 1 h and incubated with primary antibodies overnight at 4°C, followed by treatment with Fluorescence-conjugated secondary antibodies at room temperature for 1 h. Fluorescence was measured by Odyssey infrared imaging system (LI-COR Biosciences, Lincoln, USA).

Silencing of STAT3

siRNA oligonucleotides against STAT3 gene (CCGTGGAACCATACACAAA), which has been validated in previous study[15], and negative control siRNA (Sigma, St.Louis, MO, USA) were transfected into MM cells at a final concentration of 50 nM by using Lipofectamine 2000 transfection reagent (Invitrogen, Carlsbad, CA, USA), respectively.

Overexpression of STAT3 in MM cell lines

Plasmid vector was a generous gift from Dr. Houcai Wang (Tongji University). Recombinant lentivirus vectors and empty lentivirus vectors were packaged by HEK 293T cells through calcium phosphate transfection by using the lentivirus expression plasmid, psPAX2 packaging plasmid, and pMD2.G envelop plasmid. The supernatant containing lentivirus was harvested after 48 h of transfection and filtered using 0.45 μm cellulose acetate filter. Lentivirus was used for infection of MM cells in the presence of 5 μg/mL polybrene (Sigma-Aldrich). Infected MM cells expressed green fluorescent protein (GFP) and were sorted using a fluorescence activated cell sorter (FACS).

Enzyme-linked immunosorbent assay (ELISA)

MM.1S cells were cultured with BMSCs and then treated with DCZ3301 (0-1 μM) for 12, 24 or 48 h. After that, the culture supernatants were harvested and stored at -80°C until measurement. Cytokines (IL-6 and VEGF) were measured with commercially available human ELISA assay kits for IL-6 and VEGF (R&D Systems, Minneapolis, MN, USA) according to the manufactures' protocols. All measurements were carried out in duplicate.

Mouse xenograft model

Nude mice (4 to 6 weeks old) were obtained from the Shanghai Laboratory Animal Center (Shanghai, China). All animal studies were approved by the Institutional Review Board of Shanghai Tenth People's Hospital, Tongji University. Mice were injected subcutaneously with 1 x 10^6 MM.1S cells. When tumors were measurable, mice were randomly divided into treatment and control groups, each group with 5 mice. In the treatment group, mice received 30 mg/kg DCZ3301 via tail vein three times weekly for 21 days. The vehicle control group received PBS containing 1% DMSO. Tumor size and mouse body weight were monitored three times

weekly for 21 days. Tumor volume (mm^3) was calculated as 1/2 ×(relatively shorter diameter)^2× (relatively longer diameter).

Statistical analysis

Statistical significance was determined by Student's t-test. A value of $p < 0.05$ was considered significant. The combination index (CI) values were calculated by median dose effect analysis using a commercially available software program (CalcuSyn; Biosoft).

Results

DCZ3301 displayed potent cytotoxicity against multiple human cancer cell lines

DCZ3301 is a novel aryl-guanidino compound with molecular weight of 464.0 (Figure 1A). We first evaluated the effect of DCZ3301 by *in vitro* proliferation assays against nine human cancer cell lines. The results are summarized in Table 1. We further performed these assays on a panel of MM cell lines (MM.1S, NCI-H929, U266, OCI-My5, OPM2, ARP1, RPMI-8226, and 8226-R5) in the presence of increasing doses of DCZ3301 (0-16 μM). DCZ3301 induced a dose-dependent cytotoxicity in all cell lines (Figure 1B). We also treated MM.1S and RPMI-8226 cells with DCZ3301 (0-16 μM) for 24, 48 and 72 h and observed that DCZ3301 decreased cell viability in a time-dependent manner (Figure 1C and D). Moreover, DCZ3301 induced a dose-dependent cytotoxicity in $CD138^+$ MM cells isolated from BMMCs of three MM patients (Figure 1E and supplementary Fig. S1). In contrast, DCZ3301 did not induce significant cytotoxicity in co-isolated $CD138^-$ cells from MM patients, in PBMCs from three normal volunteers at concentrations as high as 32 μM, nor in stimulated $CD19^+$ human B cells (Figure 1F, G, and H). These findings indicate that DCZ3301 is selectively cytotoxic in MM cell lines and patient MM cells.

DCZ3301 induced apoptosis and decreased ΔΨm in MM cells

We explored the mechanism of cytotoxicity using annexin V/PI staining and immunoblotting in MM cells. The data showed a dose- and time-dependent increase in annexin V-positive cells after treatment with DCZ3301 in MM.1S cells (Figure 2A). In addition, DCZ3301 induced cleavage of caspase 3, 8, and 9, as well as PARP, in MM.1S cells (Figure 2B). To determine the dependence of DCZ3301-induced apoptosis on the caspase pathway, we assessed the ability of the pan-caspase inhibitor, Z-VAD-FMK to protect against cell apoptosis. As shown in Figure 2C, Z-VAD-FMK mostly blocked DCZ3301-induced cell apoptosis as determined by annexin V-PI staining. These data demonstrate that DCZ3301 triggers caspase-dependent apoptosis in MM cells. In addition, we also found that treatment of MM.1S cells with DCZ3301 significantly decreased ΔΨm in a dose-dependent manner (Figure 2D).

Table 1. Inhibition of cancer cells proliferation by DCZ3301.

	Hepatocellular carcinoma		Thyroid carcinoma		Renal clear cell carcinoma	T-cell Leukemia	Lymphoma	Multiple myeloma	
	LM3	BEL7402	SW1736	K1	786-0	MOLT-4	NUDUL-1	OPM2	H929
IC50 (μM)	14.6	20.2	23.8	34.2	13.9	9.3	7.8	1.8	3.2

Treatment of MM cells with DCZ3301 resulted in G2/M phase arrest and downregulation of Cdc25C, CDK1, and Cyclin B1

The anti-proliferative effects of DCZ3301 were further characterized by evaluating the cell cycle of MM cells treated with DCZ3301. DNA content analyses showed a significant time- and dose-dependent accumulation of cells in the G2/M phase after treatment with DCZ3301 in MM.1S cells (Figure 3A and B). This was also observed in RPMI-8266 cells, but not non-MM cells MOLT-4, 786-0, or LM3 (supplementary Fig. S2). Treatment of MM.1S with DCZ3301 resulted in downregulation of Cdc25C, CDK1, and Cyclin B1 expression in a dose-dependent manner (Figure 3C), consistent with what has been observed after a prolonged mitotic arrest[16, 17].

DCZ3301 overcame the protective effect of the BM microenvironment on MM cells

Given that the BM microenvironment plays an important role in MM growth and survival, we explored whether DCZ3301 overcame the protective effect of the BM microenvironment on MM cells. This was done both by simulating the BM microenvironment by culturing myeloma cells in the presence of cytokine (IL-6 and VEGF) or by direct co-culture with BMSCs. Although both approaches stimulated thymidine uptake by myeloma cells, neither the cytokines (IL-6 and VEGF) nor BMSCs protected against DCZ3301-induced growth inhibition (Figure 4A and B).

Preliminary mechanistic analysis of anti-myeloma activity of DCZ3301

The Raf/MEK/ERK1/2, the PI3K/AKT, and the JAK2/STAT3 pathways are known to be important for myeloma cell proliferation and survival. In our studies, DCZ3301 likewise inhibited the phosphorylation of STAT3, ERK1/2, and AKT in a dose-dependent manner in MM.1S cells (Figure 5A).

Consistent with the results in MM.1S cells, we also observed decreased activating phosphorylation in these pathways after treatment with DCZ3301 in other two MM cell lines (NCI-H929 and U266) (Figure 5B). Additionally, DCZ3301 inhibited classical NFκB signaling in a dose-dependent manner (Figure 5C). Of note, the phosphorylation of ERK1/2, p65, AKT and STAT3 were unaffected by DCZ3301 in normal and IgM-stimulated B cells (supplementary Fig. S3). Inhibitors against ERK1/2 (U0126) and AKT (KRX-0401) did not significantly influence the efficacy of DCZ3301 compared with DCZ3301 alone (data not shown). However, knockdown of STAT3 using siRNA enhanced the efficacy of DCZ3301 compared with non-specific siRNA (Figure 5D). Further, overexpressed STAT3 protected against DCZ3301-induced cell apoptosis (Figure 5E). Together these data show that DCZ3301 inactivates several pathways and suggest that STAT3 affects DCZ3301-induced lethality in MM cells.

VEGF is an important cytokine secreted by MM cells and BMSCs. In a co-culture of MM cells and BMSCs, DCZ3301 decreased VEGF secretion in a dose-dependent fashion (Figure 5F). Previous studies[18, 19] reported that VEGF secretion can stimulate IL-6 secretion, and in turn, increased IL-6 secretion can enhance VEGF secretion. Therefore, we also examined IL-6 and found that DCZ3301 resulted in a dose-dependent decrease in IL-6 secretion (Figure 5G).

DCZ3301 was active in a xenograft model

To examine the *in vivo* activity of DCZ3301, nude mice bearing subcutaneous MM.1S cells were treated with either DCZ3301 (30 mg/kg) or vehicle control by intravenous injection every other day for 21 days. DCZ3301 treatment inhibited MM tumor growth (Figure 6A). The body weights of the mice had no significant difference between groups over the course of treatment (Figure 6B). TUNEL assays showed that DCZ3301 treatment resulted in increased cell apoptosis compared to vehicle control (Figure 6C). Consistent with the *in vitro* results, Western blot analyses showed DCZ3301 treatment inhibited the phosphorylation of STAT3 and induced cleavage of PARP in myeloma tissue, compared to vehicle control (Figure 6D).

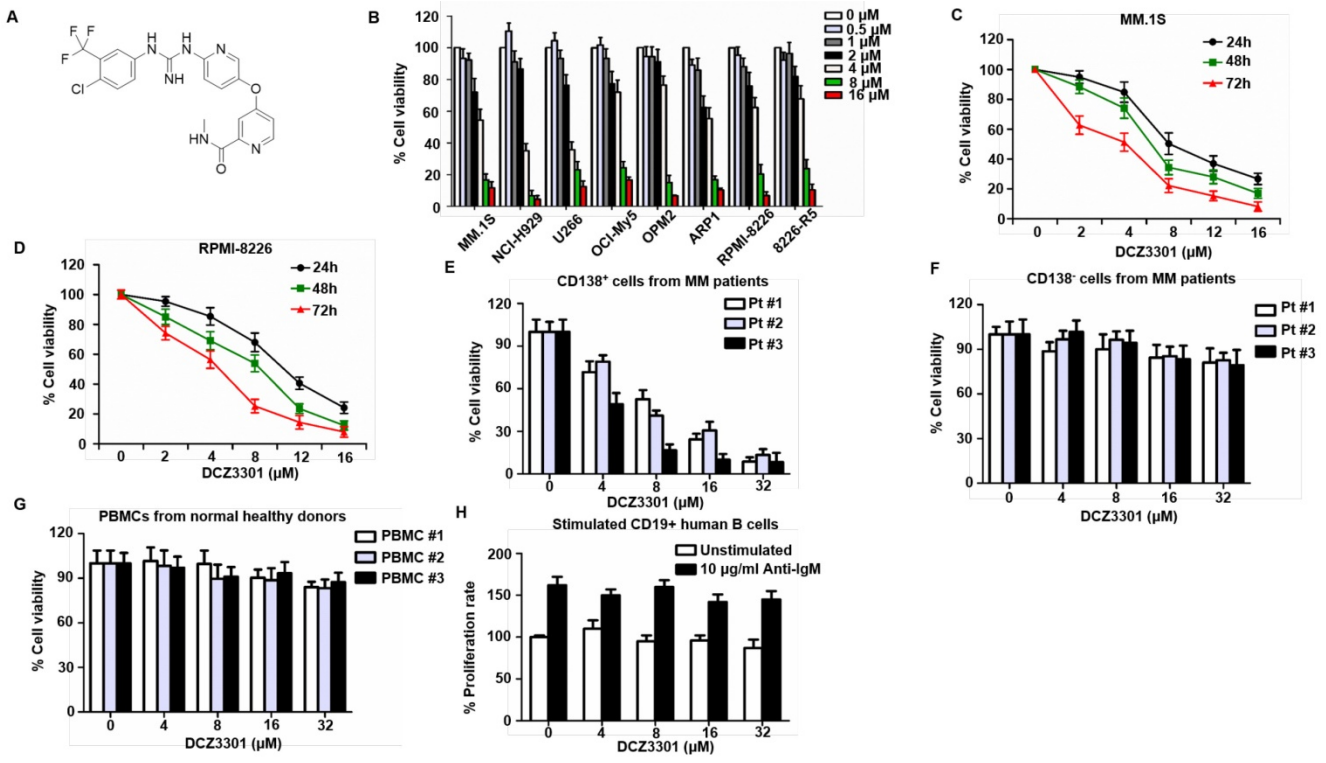

Figure 1. DCZ3301 induced cytotoxicity in MM cells. (A) Chemical structure of DCZ3301. (B) MM cell lines (MM.1S, NCI-H929, U266, OCI-My5, OPM2, ARP1, RPMI-8226 and 8226-R5) were treated with DCZ3301 (0-16 μM) for 72 h followed by assessment for cell viability. MM1S (C) and RPMI-8226 (D) were treated with DCZ3301 (0-16 μM) for 24, 48 or 72 h, then cell viability was assessed. (E) Purified patient MM cells ($CD138^+$) were treated with DCZ3301 (0-32 μM) for 48 h. Normal bone marrow mononuclear cells (BMMCs) ($CD138^-$) from three MM patients (F) or peripheral blood mononuclear cells (PBMCs) (G) from three normal volunteers were treated with DCZ3301 (0-32 μM) for 48 h then cell viability was assessed. (H) $CD19^+$ B lymphocytes were cultured in 96-well plates at 5×10^5 cells/well in RPMI 1640 medium. BCR stimulation was performed by adding a $F(ab')_2$ goat anti–human IgM at a final concentration of 10 μg/mL for 24 h. After that, cells were treated with DCZ3301 (0-32 μM) for 48 h then cell proliferation rate was assessed. In each case, data represent mean±SD of triplicate treatments.

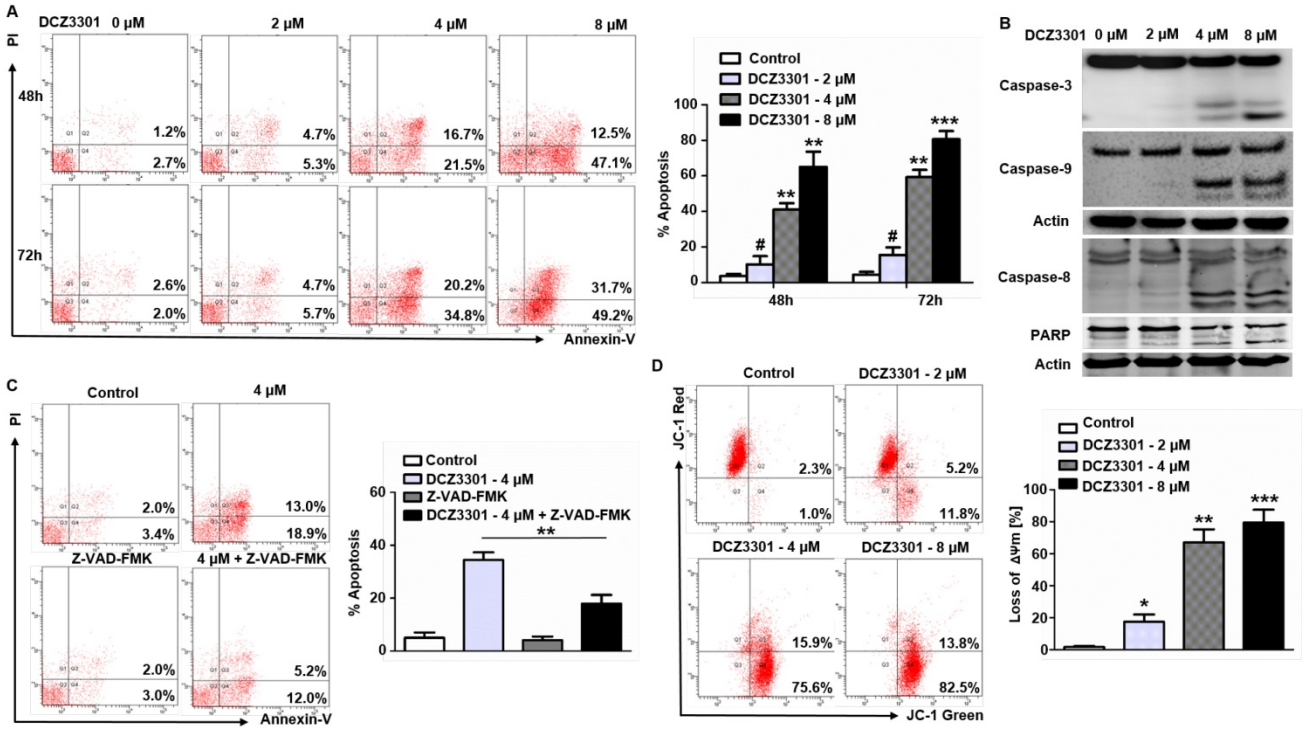

Figure 2. DCZ3301 induced apoptosis and decreased ΔΨm in MM cells. (A) MM.1S cells were treated with DCZ3301 (0-8 μM) for 48 and 72 h. Cell apoptosis was analyzed by flow cytometry using Annexin V/PI staining. Columns (right panel) represent the average percent of Annexin V positive cells from three independent experiments, which are shown as the mean±SD. (B) MM.1S cells were treated with DCZ3301 (0-8 μM) for 48 h. Whole cell lysates were subjected to western blotting using caspase 8, caspase 9, caspase 3, PARP and β-actin. (C) MM.1S cells were incubated with or without pan-caspase inhibitor Z-VAD-FMK for 1 h and then treated with DCZ3301 (4 μM) for 48 h followed by assessment of cell apoptosis using Annexin V/PI staining. Columns (right panel) represent the average percent of Annexin V positive cells from three independent experiments, which are shown as the mean±SD. (D) MM.1S cells were treated with DCZ3301 (0-8 μM) for 48 h. Mitochondrial membrane potential (ΔΨm) was analyzed by flow cytometry using JC-1 dye. Only JC-1 green positive (lower right quadrant) cells were analyzed for the loss of ΔΨm. Columns (lower panel) represent the average percent of only JC-1 green positive cells from three independent experiments, which are shown as the mean±SD. # represent $p>0.05$; * represent $p<0.05$; * * represent $p<0.01$; * * *represent $p<0.001$.

DCZ3301 synergized with bortezomib in MM cell lines and primary MM cells

To assess the rationale of using DCZ3301 as part of a combination therapy, we examined MM cell cytotoxicity of DCZ3301 in combination with bortezomib. Median dose effect analyses showed that the combination of DCZ3301 and bortezomib induced synergistic cytotoxicity, with a CI<1.0, in MM.1S, as well as MM cells from three patients (Figure 7A-D). DCZ3301 in combination with the second-generation proteasome inhibitor carfilzomib or the conventional agent melphalan, showed mixed synergistic and antagonistic results (data not shown).

Discussion

We synthesized a novel aryl-guanidino compound, DCZ3301, and found it has potent anti-cancer activity, especially against MM. Our data showed that DCZ3301 has a potent inhibitory effect on MM cell lines and primary human myeloma cells. The lack of cytotoxicity in normal PBMCs, BMMCs, and activated peripheral blood B cells even at drug concentrations of 32 μM, suggests selective cytotoxicity against tumor cells and a favorable therapeutic index for DCZ3301. Consistent with these findings, DCZ3301 had marked efficacy without any significant toxicity, such as body weight loss, in a MM xenograft mouse model.

Anti-MM activity of DCZ3301 was associated with induction of apoptosis and growth arrest. DCZ3301-triggered apoptosis was associated with the loss of mitochondrial membrane potential and activation of caspases and PARP, whereas addition of a pan-caspase inhibitor attenuated DCZ3301-induced MM cell death. The DCZ3301-induced G2/M phase arrest was associated with downregulation of Cdc25C, CDK1 and cyclin B1, which is consistent with slippage through mitotic arrest and associated induction of apoptosis[17]. Clearly there is something unique about this arrest in the MM cells, as non-MM cells did not arrest in the same phase. However, our data strongly suggest that the increased cytotoxic potency of DCZ3301 in MM cells is likely do to a combination of the ability of this drug to suppress cell cycle progression and inhibit multiple survival pathways that are known to be active in MM.

The provocation toward apoptosis is enhanced by the many pathways that are inhibited when MM cells are treated with DCZ3301. The

Raf/MEK/ERK1/2, the PI3K/AKT, the JAK2/STAT3, and NFκB survival and proliferative signaling pathways are known to be active in MM. Our results showed that DCZ3301 reduced activity in all of these pathways and did so in all three MM cell lines examined. Given that VEGF is an important cytokine secreted by MM cells and BMSCs, that VEGF secretion can stimulate IL-6 secretion, and that IL-6 can activate the JAK2/STAT3, PI3K/AKT and ERK1/2 signal pathways to trigger MM cell proliferation and survival [9-11, 19], the effect of DCZ3301 on VEGF and IL-6 secretion was explored. We found that DCZ3301 decreased VEGF and IL-6 secretion in a co-culture system containing myeloma cells and BMSCs, suggesting that reducing the level of these cytokines is one way in which DCZ3301 limits MM cell survival and proliferation. Overexpression of STAT3 signaling did not completely abrogate DCZ3301-mediated apoptosis, suggesting that the other pathways are also important in yet unexplored ways.

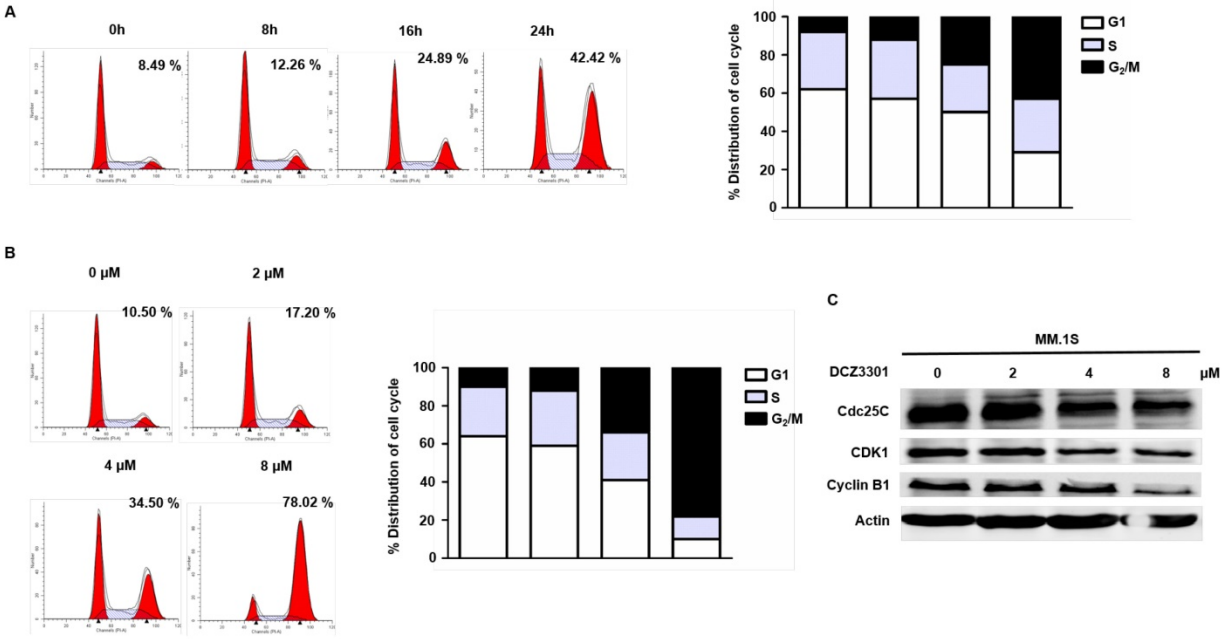

Figure 3. DCZ3301 induced G2/M phase arrest in MM cells. (A) MM.1S cells were treated with 4 μM DCZ3301 for indicated times. Cell cycle was analyzed by flow cytometry using PI staining. Bar graph shows percentage of cell populations in G1, S or G2/M phase of cell cycle. (B) MM.1S cells were treated with indicated concentrations of DCZ3301 for 24 h. Cell cycle was analyzed by flow cytometry using PI staining. Bar graph shows percentage of cell populations in G1, S or G2/M phase of cell cycle. Numerical percentage shown indicates G2/M population. (C) After treatment as in B, the expression of Cdc25C, CDK1, Cyclin B1 and β-actin were monitored by western blot.

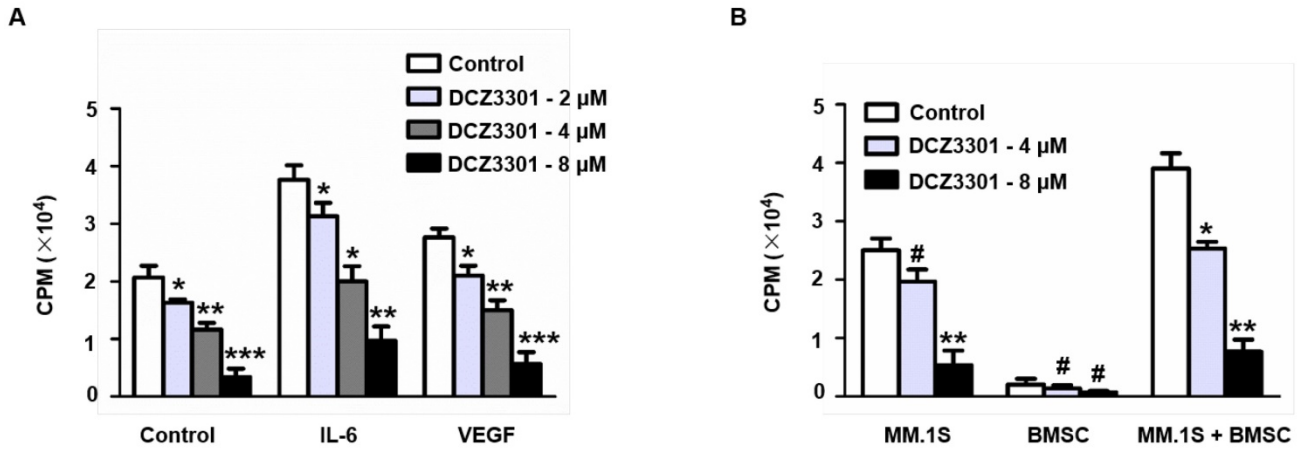

Figure 4. DCZ3301 overcame growth stimulatory effects of IL-6, VEGF, and BMSCs. (A) MM.1S cells were treated with indicated concentrations of DCZ3301 for 48 h in the presence or absence of IL-6 (10 ng/ml) and VEGF (50 ng/ml). (B) MM.1S cells, patient BMSCs, or both MM.1S and BMSCs were treated with indicated concentrations of DCZ3301 for 48 h. Cell proliferation was measured by thymidine uptake. # represent $p>0.05$; * represent $p<0.05$; * * represent $p<0.01$; * * *represent $p<0.001$.

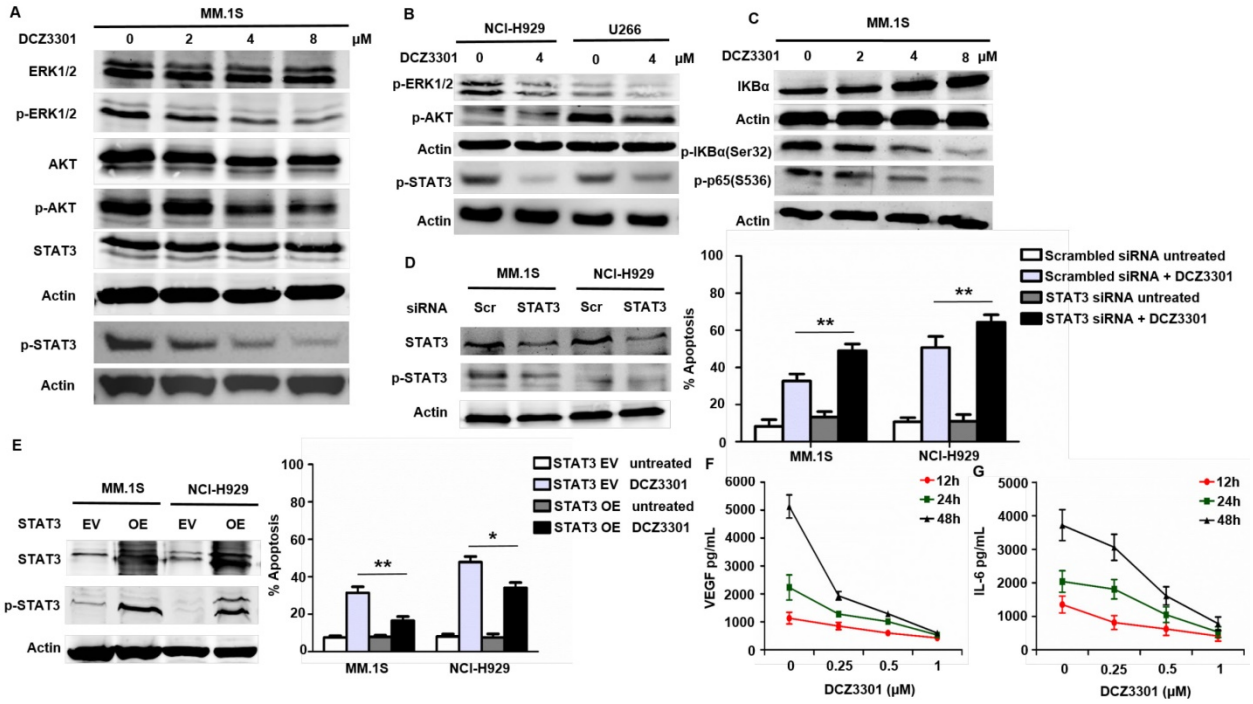

Figure 5. Mechanisms of anti-myeloma activity of DCZ3301. (A) MM.1S cells were treated with indicated concentrations of DCZ3301 for 48h. Whole cell lysates were subjected to western blotting using ERK1/2, p-ERK1/2, AKT, p-AKT, STAT3, p-STAT3 and β-actin. (B) NCI-H929 and U266 cells were treated with 4 μM DCZ3301 for 48 h. Whole cell lysates were subjected to western blotting using p-ERK1/2, p-AKT, p-STAT3 and β-actin. (C) MM.1S cells were treated with indicated concentrations of DCZ3301 for 48 h. Whole cell lysates were subjected to western blotting using IKBα, p-IKBα(Ser32), p-p65(S536) and β-actin. (D) MM.1S cells transfected with STAT3 siRNA or scrambled sequence were treated with 4 μM DCZ3301 for 48 h. After that, cell apoptosis was monitored by Annexin V/PI staining. Inset: Relative expression of STAT3 protein in MM.1S transfected with STAT3 siRNA and scrambled sequence. (E) MM.1S cells transfected with plasmid DNA containing STAT3 or empty vector were treated as in D, then cell apoptosis was monitored by Annexin V/PI staining. Inset: Relative expression of STAT3 protein in MM.1S transfected with plasmid DNA containing STAT3 or empty vector. MM.1S cells were grown in co-culture with bone marrow stromal cells (BMSCs) and then treated with DCZ3301 (0-1 μM) for 12, 24 and 48 h. After that, VEGF (F) or IL-6 (G) levels in the culture supernatants were measured using enzyme-linked immunosorbent assay (ELISA). * represent $p<0.05$; * * represent $p<0.01$.

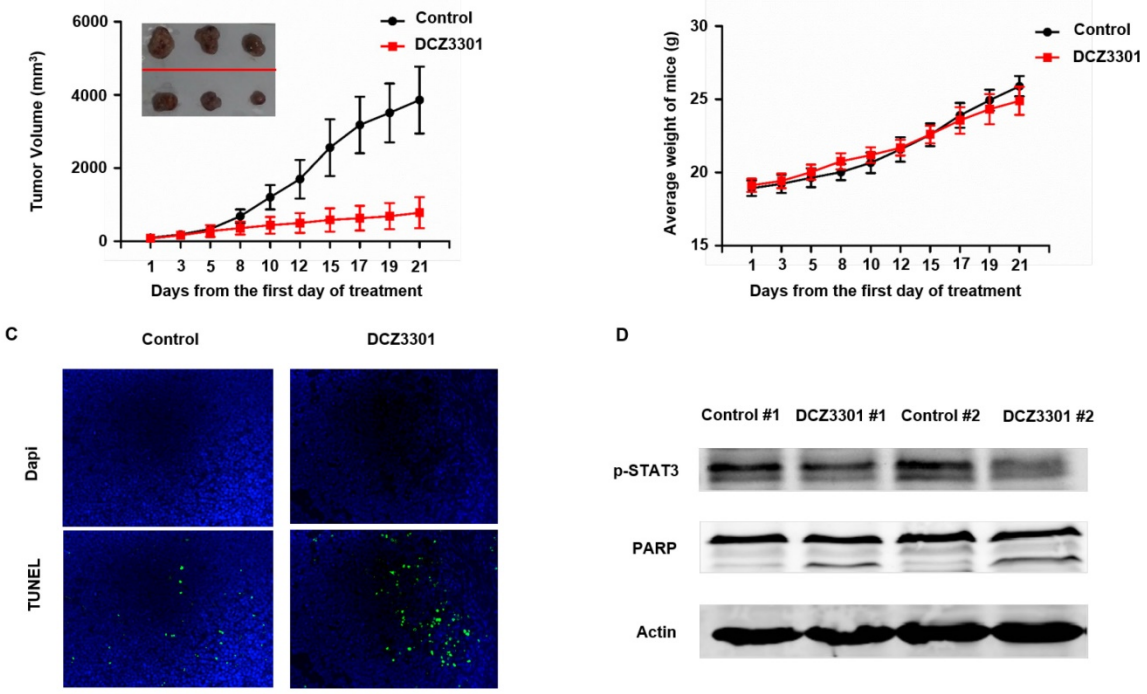

Figure 6. DCZ3301 was active in an MM xenograft model. (A) Nude mice bearing subcutaneous MM.1S tumors were treated with either DCZ3301 (30 mg/kg; intravenous) or vehicle control three times weekly for 21 days. Average and standard deviation of tumor volume (mm^3) is shown versus time when tumor was measured by caliper (mean tumor volume±SD, 5 mice/group). (B) The weight of mice was measured three times weekly for 21 days, and data represent mean±SD. (C) Tumor sections from vehicle control- and DCZ3301-treated mice were stained with FITC-dUTP as described in materials and methods (×200). (D) Tumor samples were homogenized and lysed. The extracted proteins were subjected to western blot using p-STAT3, PARP and β-actin.

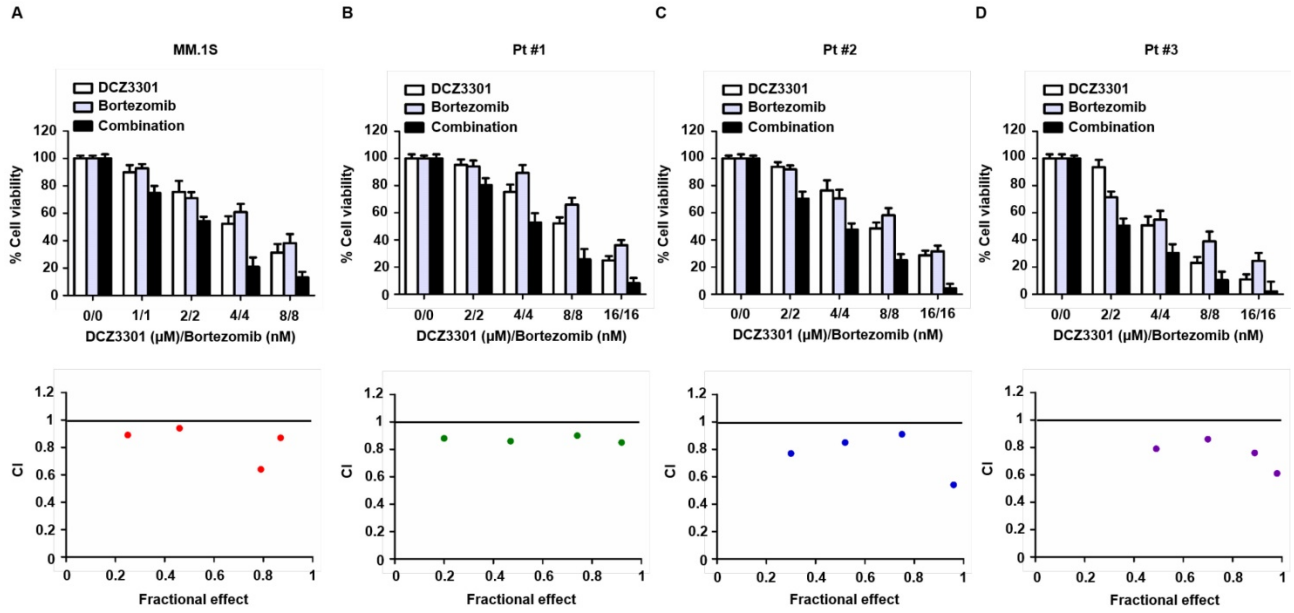

Figure 7. DCZ3301 demonstrated synergistic activity with bortezomib in MM cell lines and primary MM cells. MM.1S (A) and patient MM cells (B-D) were treated with DCZ3301, bortezomib or DCZ3301 plus bortezomib for 48 h then assessed for cell viability using CCK-8 assay. Median dose effect analysis shows the synergistic anti-MM activity of DCZ3301 and bortezomib. Combination index (CI) <1 indicates synergy.

It is well established that the BM microenvironment confers resistance to anti-MM agents[20, 21]. Therefore, the therapeutic challenge is to inhibit MM cells in the BM microenvironment. In our study, DCZ3301 induced MM cytotoxicity in the presence of IL-6, VEGF, and BMSCs, indicating that DCZ3301 may inhibit MM growth in the BM microenvironment. Previous studies reported that inhibition of IL-6/STAT3 signaling failed to induce apoptosis when MM cells were co-cultured with BMSCs[22]. The investigators suggested that BMSCs render MM cells IL-6/STAT3 independent, and it has been further suggested that combined disruption of IL-6/STAT3 and ERK1/2 signaling is required to inhibit MM cells in the presence of BMSCs[23]. Our findings are consistent with this data. We showed that DCZ3301 cannot only inhibit both ERK1/2 and STAT3 activity in MM cells, but it also can suppress proliferation in the presence of BMSCs or of exogenous IL-6 and VEGF, products in the BM microenvironment. These data provide support for the notion that DCZ3301 can suppress proliferation in the BM microenvironment.

We examined anti-MM activity of DCZ3301 in an MM xenograft mouse model. Our data showed that DCZ3301 not only inhibits tumor growth but also is well tolerated in mice. No apparent toxicity was observed in the DCZ3301 treatment group. In agreement with our *in vitro* data, downregulated STAT3 phosphorylation and increased cleavage of PARP were observed in tumor samples obtained from mice treated with DCZ3301 *in vivo*.

We assessed whether DCZ3301 could be used as part of a combination therapy and found that combining DCZ3301 with bortezomib induced synergistic anti-MM activity. Importantly, this combination was effective not only in MM cell lines but also in primary MM patient samples. Bortezomib is one of the most common myeloma agents, but dose-limiting toxicities and the development of resistance limits its long-term utility[24]. Therefore, the combination of DCZ3301 with bortezomib may be a promising therapeutic strategy to further improve patient outcome in MM. Further insight into the *in vivo* efficacy of DCZ3301 in combination with bortezomib and the mechanism of synergism is being explored in our lab.

In summary, our preclinical studies demonstrate potent *in vitro* and *in vivo* anti-MM activity of DCZ3301. These studies provide the proof-of-concept necessary to move the evaluation of DCZ3301 either alone or in combination with bortezomib to the clinic as a potential novel therapy to improve patient outcome in MM.

Supplementary Material

Supplementary figures.
http://www.thno.org/v07p3690s1.pdf

Acknowledgements

This study was supported by Grants from the National Natural Science Foundation of China (81372391, 81570190, 81529001, 81302699, 81602515, 31271496, 81600174 and 81300443).

Competing Interests

The authors have declared that no competing interest exists.

References

1. Hideshima T, Bergsagel PL, Kuehl WM, Anderson KC. Advances in biology of multiple myeloma: clinical applications. Blood. 2004; 104: 607-18.
2. Hideshima T, Mitsiades C, Tonon G, Richardson PG, Anderson KC. Understanding multiple myeloma pathogenesis in the bone marrow to identify new therapeutic targets. Nat Rev Cancer. 2007; 7: 585-98.
3. Gertz MA, Dingli D. How we manage autologous stem cell transplantation for patients with multiple myeloma. Blood. 2014; 124: 882-90.
4. Singhal S, Mehta J, Desikan R, Ayers D, Roberson P, Eddlemon P, et al. Antitumor activity of thalidomide in refractory multiple myeloma. N Engl J Med. 1999; 341: 1565-71.
5. Richardson PG, Sonneveld P, Schuster MW, Irwin D, Stadtmauer EA, Facon T, et al. Bortezomib or high-dose dexamethasone for relapsed multiple myeloma. N Engl J Med. 2005; 352: 2487-98.
6. Palumbo A, Cavallo F, Gay F, Di Raimondo F, Ben Yehuda D, Petrucci MT, et al. Autologous transplantation and maintenance therapy in multiple myeloma. N Engl J Med. 2014; 371: 895-905.
7. Louw VJ, Louw H, Webb MJ. Autologous stem-cell transplantation for multiple myeloma. N Engl J Med. 2009; 361: 1118-9; author reply 9.
8. Uchiyama H, Barut BA, Mohrbacher AF, Chauhan D, Anderson KC. Adhesion of human myeloma-derived cell lines to bone marrow stromal cells stimulates interleukin-6 secretion. Blood. 1993; 82: 3712-20.
9. Ogata A, Chauhan D, Teoh G, Treon SP, Urashima M, Schlossman RL, et al. IL-6 triggers cell growth via the Ras-dependent mitogen-activated protein kinase cascade. J Immunol. 1997; 159: 2212-21.
10. Hideshima T, Nakamura N, Chauhan D, Anderson KC. Biologic sequelae of interleukin-6 induced PI3-K/Akt signaling in multiple myeloma. Oncogene. 2001; 20: 5991-6000.
11. Catlett-Falcone R, Landowski TH, Oshiro MM, Turkson J, Levitzki A, Savino R, et al. Constitutive activation of Stat3 signaling confers resistance to apoptosis in human U266 myeloma cells. Immunity. 1999; 10: 105-15.
12. Kharaziha P, De Raeve H, Fristedt C, Li Q, Gruber A, Johnsson P, et al. Sorafenib has potent antitumor activity against multiple myeloma *in vitro*, ex vivo, and *in vivo* in the 5T33MM mouse model. Cancer Res. 2012; 72: 5348-62.
13. Gao M, Chen G, Wang H, Xie B, Hu L, Kong Y, et al. Therapeutic potential and functional interaction of carfilzomib and vorinostat in T-cell leukemia/lymphoma. Oncotarget. 2016.
14. Gao M, Gao L, Tao Y, Hou J, Yang G, Wu X, et al. Proteasome inhibitor carfilzomib interacts synergistically with histone deacetylase inhibitor vorinostat in Jurkat T-leukemia cells. Acta Biochim Biophys Sin (Shanghai). 2014; 46: 484-91.
15. Zhu S, Wang Z, Li Z, Peng H, Luo Y, Deng M, et al. Icaritin suppresses multiple myeloma, by inhibiting IL-6/JAK2/STAT3. Oncotarget. 2015; 6: 10460-72.
16. Brito DA, Rieder CL. Mitotic checkpoint slippage in humans occurs via cyclin B destruction in the presence of an active checkpoint. Curr Biol. 2006; 16: 1194-200.
17. Gascoigne KE, Taylor SS. Cancer cells display profound intra- and interline variation following prolonged exposure to antimitotic drugs. Cancer Cell. 2008; 14: 111-22.
18. Gupta D, Treon SP, Shima Y, Hideshima T, Podar K, Tai YT, et al. Adherence of multiple myeloma cells to bone marrow stromal cells upregulates vascular endothelial growth factor secretion: therapeutic applications. Leukemia. 2001; 15: 1950-61.
19. Ramakrishnan V, Timm M, Haug JL, Kimlinger TK, Wellik LE, Witzig TE, et al. Sorafenib, a dual Raf kinase/vascular endothelial growth factor receptor inhibitor has significant anti-myeloma activity and synergizes with common anti-myeloma drugs. Oncogene. 2010; 29: 1190-202.
20. Abe M. Targeting the interplay between myeloma cells and the bone marrow microenvironment in myeloma. Int J Hematol. 2011; 94: 334-43.
21. Basak GW, Srivastava AS, Malhotra R, Carrier E. Multiple myeloma bone marrow niche. Curr Pharm Biotechnol. 2009; 10: 345-6.
22. Chatterjee M, Honemann D, Lentzsch S, Bommert K, Sers C, Herrmann P, et al. In the presence of bone marrow stromal cells human multiple myeloma cells become independent of the IL-6/gp130/STAT3 pathway. Blood. 2002; 100: 3311-8.
23. Chatterjee M, Stuhmer T, Herrmann P, Bommert K, Dorken B, Bargou RC. Combined disruption of both the MEK/ERK and the IL-6R/STAT3 pathways is required to induce apoptosis of multiple myeloma cells in the presence of bone marrow stromal cells. Blood. 2004; 104: 3712-21.
24. Chauhan D, Tian Z, Nicholson B, Kumar KG, Zhou B, Carrasco R, et al. A small molecule inhibitor of ubiquitin-specific protease-7 induces apoptosis in multiple myeloma cells and overcomes bortezomib resistance. Cancer Cell. 2012; 22: 345-58.